

See discussions, stats, and author profiles for this publication at: <https://www.researchgate.net/publication/231188875>

# Background correction for the analysis of high-solids samples by graphite furnace atomic absorption

ARTICLE *in* ANALYTICAL CHEMISTRY · DECEMBER 1977

Impact Factor: 5.64 · DOI: 10.1021/ac50022a020

---

CITATIONS

29

---

READS

12

## 2 AUTHORS:



**James Harnly**

Agricultural Research Service

**163** PUBLICATIONS **3,397** CITATIONS

SEE PROFILE



**Tom Calvin O'Haver**

University of Maryland, College Park

**81** PUBLICATIONS **1,446** CITATIONS

SEE PROFILE

# Background Correction for the Analysis of High-Solids Samples by Graphite Furnace Atomic Absorption

J. M. Harnly and T. C. O'Haver\*

Department of Chemistry, University of Maryland, College Park, Maryland 20742

**A direct absorbance read-out circuit has been built for use with an AA system consisting of a continuum source and an echelle monochromator modified for wavelength modulation (CEWM-AA). The system is shot noise limited and capable of correcting for 3.0 absorbance units of nonspecific source attenuation. Cd, Pb, and Cu are analyzed directly in 3% NaCl, serum, and urine. CEWM-AA detection limits in 3% NaCl were equivalent to or better than those for conventional background-corrected line source AA and Zeeman effect AA.**

The most commonly-used background correction technique for conventional line source AA employs a continuum source in addition to the primary elemental source. This dual source technique was first described by Koirtjohann and Pickett (1) and has subsequently been adopted by almost all manufacturers of AA instruments. Difficulty in characterizing background corrected line source AA (AAL-BC) arises from the necessity of exactly aligning the beams from two sources (2-5) and of selecting the appropriate spectral bandpass (5) and electronic gain (6). Morganthaler (7) and Hendriks-Jongerius and De Galan (4) have stated that 1.0 absorbance unit represents the maximum allowable source attenuation for AAL-BC systems. Most AAS manufacturers recommend modification of the sample or of the method of preparation if attenuation approaches this level (8, 9). Recently the dependence of the accuracy of background correction on the optimization of the various optical and electronic parameters was again stressed by Morris and Newstead (10). They reported a source attenuation limit of 1.7 absorbance units for the Pye Unicam SP2900 AAS (11) which features improved control for these parameters.

The central assumption upon which the operation of AAL-BC is based is that the average absorption measured over the monochromator spectral bandpass (typically 0.1-1 nm) is equal to the background absorption under the (much narrower) analyte atomic absorption line. This assumption is generally valid for light losses due to scattering which is smoothly wavelength dependent. However, it has been shown that AAL-BC may give inaccurate background correction (4, 12, 13) when the fine structure of the molecular background absorption or atomic absorption of the matrix falls within the spectral bandpass of the monochromator. Inaccurate results will, of course, also arise from the rarer occurrence of direct spectral overlap of atomic lines (14, 15).

The only commercially-available alternative to AAL-BC is the Hitachi Zeeman effect AA (ZAA) (16-20). Since only a single source is employed, the problem of exact beam alignment does not arise. Furthermore, the background readings are taken much closer ( $\approx 0.01$  nm) to the analyte line. Accurate correction for attenuation of 1.7 absorbance units has been reported. With the magnetic field around the source, the selection of spectral lines is limited somewhat by the magnetically induced fine structure of the source line (18). This problem appears to have been solved by placing the magnetic field around the atomization source (19, 20). However, a new uncertainty arises concerning the magnetically

induced fine structure in the absorption spectrum of metallic components of the sample.

Conceptually, the simplest means of correcting for background spectral interferences in atomic absorption is the use of wavelength modulation in conjunction with a continuum primary source. Such a system, employing a medium resolution monochromator, was first described by Snelleman (21). The modulation process sweeps the absorption profile repeatedly across the exit slit, resulting in a ripple in the photo-signal which is proportional to the intensity absorbed and is independent of broad band additive interferences (22). Zander et al. (23) combined a high intensity continuum source and a wavelength modulated high resolution echelle monochromator (24). This system, dubbed CEWM-AA, has both of the essential advantages of ZAA: a single source is used and only the narrow spectral region near the analyte line is examined. Moreover, the single source suffices for all elements. A useful feature of this system is that the photomultiplier output and the wavelength modulation waveform may be combined to give a real-time  $x$ - $y$  oscilloscope display of the absorption spectrum near the analyte line. Nonspecific source attenuation and spectral line overlap can be visually detected.

In the simplest sense the background correction capabilities of wavelength modulation with a continuum source (WM-AAC) assumes an unstructured background over the modulation interval. However, the technique has also been used to correct for more complex spectral interferences. Koirtjohann et al. (25), using square wave modulation, have measured emission peaks in highly structured background. Epstein and O'Haver (26) and Sydor and Hieftje (27) used wavelength modulation to compensate for spectral overlap interferences in atomic emission. Zander et al. (15) demonstrated that CEWM-AA is capable of correcting for all major types of spectral interferences in atomic absorption, including direct spectral overlaps with separation as little as 0.003 nm.

The calculation of absorbance for WM-AAC is not straightforward. Snelleman (21) used the log of the ac component as an approximation of absorbance. This convention has been employed by more recent researchers investigating a variety of WM-AAC systems (28-30). The approximation is valid provided that the analyte absorption is small and that the source attenuation is sufficiently small that  $I_0$  and  $I_0 - I$  do not decrease by more than a few percent. These criteria tend to exclude most real-world samples.

Zander et al. (23) were the first to attempt to calculate true absorbance values using the CEWM-AA system. These calculations were based on separate measurements of  $I_0$  and  $I_0 - I$ . Absorbances for samples causing significant source attenuation could not be calculated as there was no means of determining  $I_0$  during atomization. Hager (22) has shown that a ratioing of the ac component (proportional to  $I_0 - I$ ) to the dc component (proportional to  $I_0$ ) will produce a signal which is dependent only on the analyte concentration and is independent of the source intensity.

This paper will describe an electronic circuit for the real-time ratioing of the ac signal to  $I_0$ . This circuit, used with the CEWM-AA system, results in an instrument which: (1)

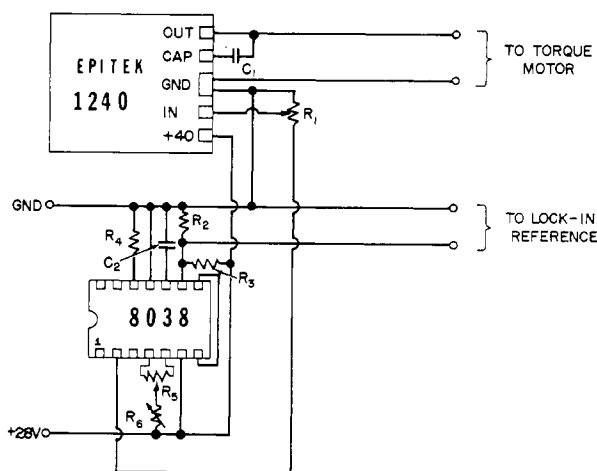


**Figure 1.** Waveform generator circuit.  $C_1 = 1000 \mu\text{F}$ ;  $C_2 = 0.15 \mu\text{F}$ ;  $R_1 = 0\text{--}100 \text{ k}\Omega$ ;  $R_2$  and  $R_3 = 100 \text{ k}\Omega$ ;  $R_4 = 82 \text{ k}\Omega$ ;  $R_5$  and  $R_6 = 0\text{--}10 \text{ k}\Omega$

gives a real-time absorbance read-out, continuously corrected for source attenuation; (2) using only a single source, gives capabilities exceeding those of a double beam system; and (3) has reduced the overall system noise level to the shot noise limit.

The source attenuation limits for the CEWM-AA system will be defined and the operating characteristics will be described. To demonstrate the system's capability to handle real samples, Cd, Pb, and Cu are analyzed in 3% NaCl, blood serum, and urine. These matrices have been selected because of their well documented spectral interferences (31–37). The background correction capabilities of the CEWM-AA system will be compared to those of existing commercial AA systems whenever possible.

## EXPERIMENTAL

The CEWM-AA system has been described (15). For these studies, an Eimac 300-W Xe "VIX-UV" continuum lamp (PS. 300-1 Eimac Power Supply, Varian Eimac Div., San Carlos, Calif.) was substituted for the 150-W Eimac lamp used previously. The lamp was run at 15 A in the continuous mode. An improved Model 102 echelle monochromator (Spectrametrics, Inc., Andover, Mass.) was used. The newer model provided greater order separating dispersion resulting in less stray light due to order overlap.

The monochromator was modified for wavelength modulation by placing a quartz refractor plate (1 inch  $\times$  1 inch  $\times$   $\frac{1}{8}$  inch) mounted on a torque motor (Model S4-075B, MFE, Salem, N.H.) approximately 10 cm behind the entrance slit. The refractor plate was modulated sinusoidally at 80 Hz using an integrated circuit waveform generator and a modular audio amplifier (Model 1240, Epitek Electronics, Ltd., Ottawa, Canada). This circuit is shown in Figure 1. Entrance and exit slits 25  $\mu\text{m}$  wide and 300  $\mu\text{m}$  high were used at all times, except where noted.

The atomization source was either a Perkin-Elmer HGA 2000 or the burner assembly from a Varian Techtron AA-4. For the flame configuration, an air-acetylene flame was used with a Techtron AB-41 (10-cm slot) burner head and a Techtron GCU-2 gas control unit (Varian Techtron, Melbourne, Australia).

**Direct Absorbance Read-Out Circuit.** In a conventional double-beam atomic absorption spectrophotometer, absorbance is derived from measurements of the incident and transmitted intensities,  $I_0$  and  $I$ , respectively. Both  $I_0$  and  $I$  are assumed to be measured at the same wavelength, the difference being that the  $I_0$  measurement is made by utilizing optical components (mirrors, etc.) which bypass the primary beam around the atomizer. In the CEWM-AA system described here, on the other hand,  $I_0$  is defined as the intensity of the primary beam transmitted through the atomizer at a wavelength just off the analyte absorption line, while  $I$  is defined as before. This definition of  $I_0$  is identical to the conventional one if the analyte does not absorb at the wavelength where  $I_0$  is measured, if the

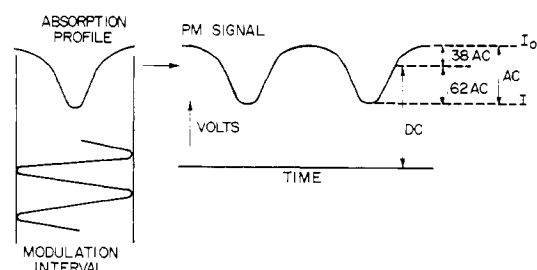


**Figure 2.** Photomultiplier output signal for the CEWM-AA system showing analyte absorption

source-monochromator-detector response changes insignificantly over the wavelength modulation interval and if there is no nonspecific source attenuation. The first two conditions are easily ensured by the proper choice of modulation interval (typically about 0.01 nm). The particular advantage of this new definition of  $I_0$ , however, is that nonspecific source attenuation has no effect on the ratio of  $I_0$  to  $I$ , since both  $I_0$  and  $I$  are transmitted through the atomizer and are attenuated by the same factor. The only requirement is that the source attenuation be the same at the wavelengths where  $I$  and  $I_0$  are measured, which is generally the case since the modulation interval is only about 0.01 nm. Thus, by defining  $I_0$  in this way, we obtain all the benefits of double-beam and background corrected operation with a much simpler optical system.

Sinusoidal wavelength modulation across an isolated atomic absorption line produces a ripple or ac component in the photomultiplier signal as shown in Figure 2. This waveform represents a convolution of the modulation waveform, the atomic absorption profile, and the monochromator slit function as has been described mathematically by O'Haver et al. (38). The photomultiplier signal consists of an ac signal superimposed on a dc signal. With a sufficiently large modulation interval, the upper limit of the ac component corresponds to  $I_0$  and the lower limit to  $I$ , as shown in Figure 2. In this manner, the average  $I_0$  value actually represents the average of source intensities measured just off both sides of the analyte line. Using these values, absorbance can be calculated in the normal manner.

The easiest way to accomplish the absorbance computation electronically is to measure the ac and dc component independently. Let us consider the case of sinusoidal modulation of a Gaussian profile at the optimum modulation interval. Using a numerical integration procedure similar to that described by O'Haver et al. (38), it can be shown that  $I_0$  equals the dc component plus 38% of the peak-to-peak ac component and  $I$  equals the dc component minus 62% of the ac component (Figure 2). The absorbance is:

$$ABS = \log \left( \frac{I_0}{I} \right) = \log \left( \frac{DC + 0.38 AC}{DC - 0.62 AC} \right) \quad (1)$$

where AC and DC are the peak-to-peak ac component and dc component, respectively.

The measurement of DC is straight-forward using a low pass filter. The value of AC is determined using a lock-in amplifier. It can be shown (Equation 18 of reference 38) that the lock-in output,  $E_L$ , is 0.274 of the peak-to-peak voltage of the input signal:

$$E_L = 0.274 AC \quad (2)$$

Moreover, the lock-in will amplify the signal by some factor  $M$  depending on which sensitivity range is used. Thus we can write:

$$AC = \frac{E_L}{0.274 M} \quad (3)$$

In order to prevent overload of the lock-in input circuit, it is necessary to attenuate the input signal by a factor,  $R$ . Taking this factor into account:

$$AC = \frac{RE_L}{0.274 M} \quad (4)$$

Combining Equations 1 and 4 gives:

$$ABS = \log \left( \frac{DC + \left[ \frac{0.38 R}{0.274 M} \right] E_L}{DC - \left[ \frac{0.62 R}{0.274 M} \right] E_L} \right) = \log \left( \frac{DC + K_1 E_L}{DC - K_2 E_L} \right) \quad (5)$$

where the  $K$ 's represent the terms in brackets.

Figure 3 shows a block diagram of the electronic circuit which solves Equation 5. All op amps are National Semiconductor type LM 316H. The log ratio module is an Infotronics LR 101. The lock-in amplifier is a Princeton Applied Research Model 128.

A 1 M $\Omega$  resistor ( $R_1$ ) serves as the photomultiplier load. Op amp No. 1 is used as a pre-amp to increase the signal voltage to close to 10 V (maximum voltage rating of op amp output). The signal is then applied through a voltage divider to the lock-in amplifier and to the low pass filter (op amp No. 2). A lock-in output time constant of 0.3 s was selected (0.1 s proved too small to adequately filter the ac component at the low pass filter, op amp No. 2). This time constant was closely matched at the low pass filter (op amp No. 2) in order to avoid transient signals which can arise from a mismatch of the numerator and denominator time constants in a ratio system (10).

The lock-in amplifier is tuned to twice the wavelength modulation frequency. The reference signal is provided by the 8038 waveform generator (Figure 1). The lock-in's front-end high pass filter is used in the "50 Hz" position to avoid "OVERLOAD" situations from occurring with sudden changes in  $I_0$  caused by source attenuation during the ash or atomization cycle. Even using the least sensitive scale, "250 mV", the lock-in input is overloaded for samples with no background attenuation and high atomic absorption. With  $I_0$  adjusted to 10 V, the maximum possible value for AC is 10 V. The lock-in is capable of handling only 0.9 V peak-to-peak (0.250 V/0.274). Consequently, a voltage divider must be used to decrease AC by a factor of 11 ( $R = 11$ ). In this least sensitive scale, 0–250 mV on the front meter is amplified by a factor of 4 ( $M = 4$ ) at the output connector. Thus  $E_L$  will vary from 0 to 1 V.

Op amp No. 3, 4, and 5, combine DC and  $E_L$  as shown in Equation 5. Op amp No. 4 performs the numerator addition while No. 3 and 5 perform the denominator subtraction. With  $R = 11$  and  $M = 4$ ,  $K_1$  and  $K_2$  are 3.81 and 6.22, respectively. These factors define the ratio of the resistor values at op amp No. 4 and 3 (100 k $\Omega$ /26.2 k $\Omega$  = 3.81, 100 k $\Omega$ /16.05 k $\Omega$  = 6.22). Absorbances computed by this circuit were found to agree with those calculated from direct measurements of  $I$  and  $I_0$  estimated from the oscilloscope display of the photosignal.

The log ratio module computes absorbance based on the input  $I_0$  and  $I$  values. This module enters a failure mode if its input voltages drop below 6 mV. The limits of analyte atomic absorption are therefore given by the equation:

$$ABS = \log \left( \frac{I_0}{0.006} \right) \quad (6)$$

Assuming  $I_0$  has been adjusted to 10 V initially the attenuation would be:

$$SOURCE \text{ ATTENUATION} = \log \left( \frac{10}{I_0} \right) \quad (7)$$

Combining the two gives:

$$ABS + ATTENUATION = \log \left( \frac{10}{0.006} \right) = 3.22 \quad (8)$$

We would therefore predict that we could tolerate a background absorbance of about 3 absorbance units at low analyte atomic absorbances. Higher analyte absorbances limit the source attenuation that can be tolerated; however dilution of the sample would then become feasible. If the light beam is totally blocked,

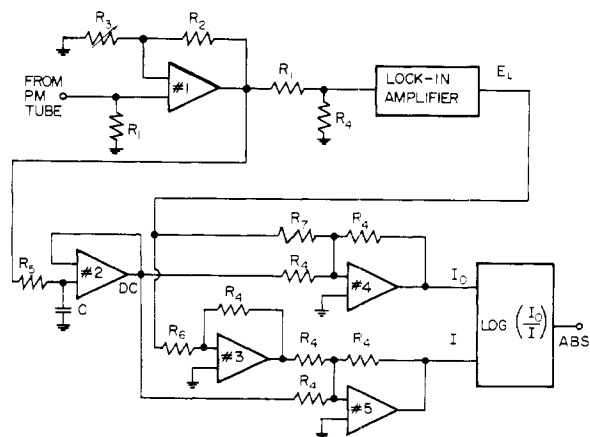


Figure 3. Circuit for direct absorbance read-out for CEWM-AA.  $R_1 = 1 \text{ M}\Omega$ ;  $R_2 = 470 \text{ k}\Omega$ ;  $R_3 = 23.5 \text{ or } 470 \text{ k}\Omega$ ;  $R_4 = 100 \text{ k}\Omega$ ;  $R_5 = 2 \text{ M}\Omega$ ;  $R_6 = 16.0 \text{ k}\Omega$ ;  $R_7 = 26.2 \text{ k}\Omega$ ;  $C = 0.15 \mu\text{F}$ .  $E_L$ ,  $DC$ ,  $I_0$ , and  $I$  are defined in the text

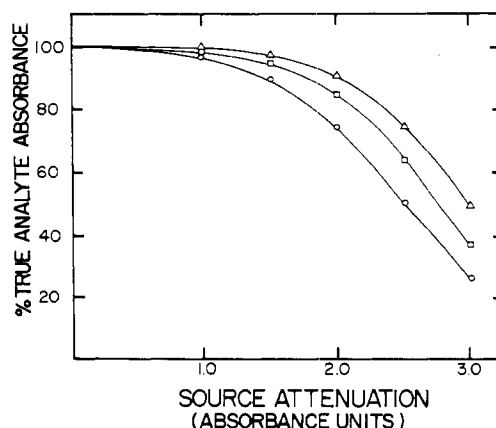


Figure 4. The effect of a 10-mV bias voltage on the accuracy of the computed analyte absorbance as a function of source attenuation. ( $\Delta$ ) 0.05 absorbance. ( $\square$ ) 0.1 absorbance. ( $\circ$ ) 1.0 absorbance

of course, the ratio operation will fail and the output goes to a 10-V limit.

The failure mode can be averted by applying a negative bias to op amp No. 2. Thus, even if the photomultiplier signal goes to zero, the same small positive voltage is seen at the  $I_0$  and  $I$  inputs to the log ratio module, and the module will continue to output zero absorbance but with a much larger noise component. Equation 5 can be rewritten:

$$ABS = \log \frac{DC + K_1 E_L + V_B}{DC - K_2 E_L + V_B} \quad (9)$$

where  $V_B$  is the bias voltage (typically 10 mV). Erroneously low absorbances will result when  $V_B$  becomes significant with respect to  $I$ . Assuming  $I_0$  to be initially adjusted to 10 V and the bias voltage to be 10 mV, Figure 4 shows the effect of source attenuation on the computed analyte absorbance. The induced error depends greatly on both analyte absorbance and source attenuation. In practice, it was found that the use of this bias voltage resulted in no practical advantage.

**Characterization of the Electronics.** To test the source attenuation tolerance of the direct absorbance read-out circuit, a steady state atomization source (air-acetylene flame) and artificially induced source attenuation were used.  $I_0$  was adjusted to approximately 10 V with the slits 25  $\mu\text{m}$  wide and 500  $\mu\text{m}$  high. Attenuation was achieved by combining the use of appropriate filters and reduction of the slit height. Analyte absorbance was introduced by aspiration of appropriate standards.

This experimental configuration did not reproduce the rapid changes in absorbance which are observed for real samples using a flameless atomization device. However, the time constants for

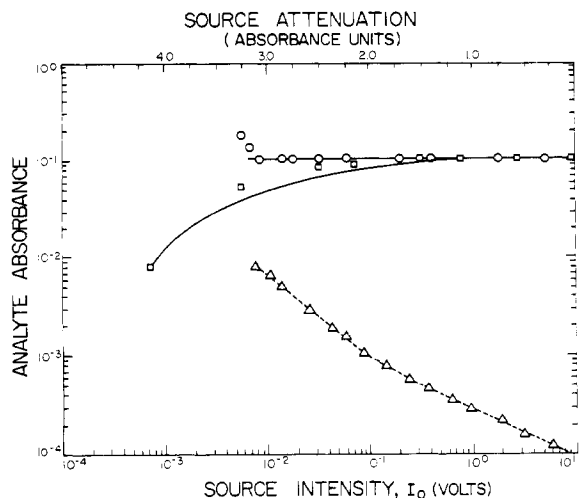


**Figure 5.** Analyte absorbance and absorbance noise as a function of source attenuation. (O) analyte absorbance, no bias voltage. (□) analyte absorbance, 10-mV bias. (Δ) absorbance noise, rms. (—) predicted analyte absorbance, with and without bias voltage. (---) straight lines fitted to absorbance noise

both branches of the circuit (*AC* and *DC*) were carefully matched as explained earlier. No transient signals were observed even when source attenuation went quickly from 0.0 to 4.0 absorbance units (the worst case).

**Analysis of High Attenuation Samples.** Cd, Pb, and Cu were analyzed in rat blood serum, fresh human urine, and 3% NaCl (reagent grade). Standards for all three elements were prepared in deionized water and in 3% NaCl solution.

Furnace temperatures for the ashing and atomizing cycle were taken from Perkin-Elmer's "Analytical Methods Using the HGA Graphite Furnace" (39). A drying temperature of 125 °C was used. The length of the drying, ashing, and atomizing cycles was 10, 30, and 8 s, respectively, for all standards and samples for all three elements.

## RESULTS AND DISCUSSION

**Characterization of the Electronics.** The ability of the electronics to handle high source attenuation was tested as described in the Experimental section. Figure 5 shows the observed (points) and predicted (solid lines) absorbance signals and the absorbance noise levels as a function of source attenuation.

With a bias of 10 mV applied to both *I* and *I*<sub>0</sub>, a longer working range is realized. However, a 5% deviation of the electronically computed absorbance from the true absorbance is observed with a source attenuation of 2.0 absorbance units. Reasonable experimental agreement with the predicted absorbance was obtained for attenuation as high as 4.0 absorbance units. The use of the method of standard additions would permit analysis of samples with source attenuation this severe, provided the increased noise levels could be tolerated. Without the bias voltage, the source attenuation limit is approximately 3.0 absorbance units for samples with analyte absorbance of 0.2 or less. Unlike the bias voltage case, the correct absorbance is computed for source attenuation from 0 to 3.0 absorbance units.

The decision whether or not to employ bias would depend on the nature of the analyte and the matrix. For samples where matrix effects cause a change in slope (multiplicative interference), the method of standard additions would be used anyway. Deviation of the computed absorbance from the true absorbance because of the electronics would have no effect on the analysis since all the method of additions samples would be expected to give the same degree of attenuation. If calibration standards were employed, no bias would be used unless it was known the source attenuation didn't exceed 2.0 absorbance units. The circuit has been built so the bias may

be turned on or off from a switch on the front panel. In both modes, the limits of attenuation are dictated by the electronics.

Figure 5 also shows that for background absorbances up to 2.0, the signal-to-noise ratio decrease with the square root of the decrease in *I*<sub>0</sub> (increase in source attenuation). This is as expected for a short noise limited system. A log-log plot of absorbance noise vs. *I*<sub>0</sub> gives a slope of -0.48 at higher intensities. The slope of -0.89 at lower intensities occurs as a result of the increased significance of the electronic noise as the *I* and *I*<sub>0</sub> inputs get closer to zero volts.

As for any shot noise limited system, the signal-to-noise ratio decreases with the square root of the decrease of the source intensity. A source attenuation of 2.0 absorbance units will be accompanied by a degradation of the detection limit by a factor of 10, regardless whether the source is attenuated by the sample matrix at a given wavelength or results from the selection of another wavelength where the Eimac source is less intense. The pre-amp or photomultiplier gain can always be increased to bring *I*<sub>0</sub> back to its original value (preserving the 3.0 source attenuation limit) but the loss in the signal-to-noise ratio cannot be reclaimed. Thus, if the rms noise at a given wavelength is known, the noise at any other wavelength is predictable from the source spectrum, and the noise during the analysis of any sample is predictable from the background attenuation. Additionally, the detection limit of any element can be calculated if the sensitivity is known.

**Analysis of High Background Samples.** To demonstrate the background correction capabilities of the CEWM-AA spectrometer using real samples, Cd, Cu, and Pb were analyzed in 3% NaCl, rat blood serum, and human urine using the Perkin-Elmer HGA 2000 graphite furnace. For each element, the furnace temperature programs recommended by the Perkin-Elmer methods manual (39) were used. Other than this, no special efforts were made to optimize sensitivity or to minimize the source attenuation. The drying and ashing stages were kept as short as possible. A 30-s ash cycle was necessary to prevent spattering of the complex matrix samples. In several cases, larger than normal sample sizes were employed to test the ability of the system to handle source attenuations much higher than normal.

Data for the analysis of Cd and Cu in the various matrices is shown in Figures 6 and 7, respectively. The upper trace in each figure shows the transmitted source intensity, *I*<sub>0</sub>, the middle trace shows the analyte absorbance signal, and the lower trace shows the background noise signal obtained for each matrix measured just off the analyte line.

The source intensity trace shows the *I*<sub>0</sub> value that is used in the analyte absorbance computation at each point in the analysis. Any decrease in the source intensity is a result of attenuation of the source by the matrix. As can be seen for the Cd data in Figure 6, even though only 20 μL sample sizes were used, considerable attenuation of the source occurred. The peak source attenuation is approximately 1.8, 2.0, and 2.0 absorbance units for 3% NaCl, serum, and urine, respectively. This degree of attenuation is greater than that observed for similar sample sizes at longer wavelengths (e.g., for Cu in Figure 7) and undoubtedly reflects the increased scatter and molecular absorption expected in the UV.

Despite the large attenuation of the source, clearly defined Cd absorbance peaks are readily seen in 3% NaCl and urine (there is no detectable Cd in rat blood serum). No difference in the analyte absorbance was noted for either the 3% NaCl or urine matrix when a 10-mV electronic bias voltage was applied. Since the source attenuation is close to 2.0 absorbance units, this indicates the analyte peak didn't occur at the point of maximum attenuation. A close comparison of the position of the absorbance peaks to the source attenuation reveals the Cd is volatilized a short time before the main background

Table I. Detection Limits for Cd in Complex Matrices

Matrix	Concn, ppb	Abs.	mAbs/pg <sup>a</sup>	Noise, p-p, Abs.	Det. limit	
					ppb	pg <sup>a</sup>
H <sub>2</sub> O	1	0.018	0.90	0.008	0.2	4
3% NaCl	10	0.140	0.70	0.070	2.0	40
Serum	... <sup>b</sup>	...	...	0.062	...	...
Urine	9.2 <sup>c</sup>	0.155	0.82	0.046	1.1	22
Beam blocked	...	...	...	0.105	...	...

<sup>a</sup> Based on 20- $\mu$ L sample size. <sup>b</sup> No Cd detectable in rat blood serum. <sup>c</sup> Determined by method of standard additions.

Table II. Detection Limits for Cu in Complex Matrices

Matrix	Sample size, $\mu$ L	Concn, ppb	Abs.	mAbs/pg	Noise p-p, Abs	Det. limit	
						ppb	pg
H <sub>2</sub> O	20	10	0.012	0.060	0.001	0.3	6.7
	100	10	0.047	0.047	0.001	0.1	8.5
3% NaCl	20	10	0.005	0.025	0.003	2.4	48
	100	10	0.013	0.013	0.0072	2.2	222
Serum	20	1640 <sup>a</sup>	0.569	0.017	0.001	1.2	20
	100	1640	1.22	0.007	0.006	3.2	323
Urine	20	19.5 <sup>a</sup>	0.023	0.059	0.002	0.7	14
	100	19.5	0.054	0.028	0.0035	0.5	51

<sup>a</sup> Determined by method of standard additions.

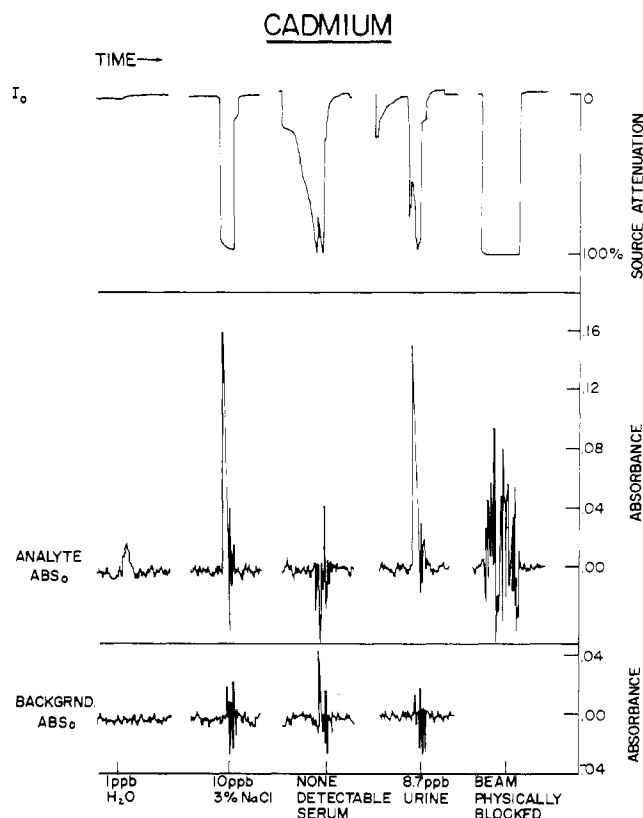


Figure 6. Traces of  $I_0$ , analyte absorbance, and background absorbance noise (off the line) for the analysis of Cd in H<sub>2</sub>O, 3% NaCl, serum, and urine (20- $\mu$ L sample size)

component. The method of standard additions was used to determine the Cd concentration in urine (9.2 ppb) and to verify that the suppression of 1.0 ppb Cd in 3% NaCl was a matrix effect.

The background noise trace (bottom of Figures 6 and 7) is obtained by tuning the monochromator 0.01 to 0.02 nm to one side of the analytical line and repeating the analysis. This is meaningful because of the use of the continuum primary source. At this offset wavelength, there can be no analyte

Table III. Detection Limits for Pb in Complex Matrices

Matrix	Concn, ppb	Abs.	mAbs/pg <sup>a</sup>	Noise p-p, Abs	Det. limit	
					ppb	pg
H <sub>2</sub> O	50	0.052	0.052	0.0028	1.0	22
3% NaCl	50	0.049	0.049	0.0123	5.0	100
Serum	... <sup>b</sup>	...	...	0.0103	...	...
Urine	... <sup>b</sup>	...	...	0.0092	...	...

<sup>a</sup> Based on 20- $\mu$ L sample size. <sup>b</sup> No Pb detectable.

absorbance; however, the source attenuation of the matrix remains very nearly the same. In fact, from the scope display of the spectrum, it was clear that there was no resolvable fine structure within the 0.01-nm modulation interval. The background signals shown in Figure 6 result from the increased noise levels as the source intensity is attenuated by the sample.

The applicability of the concept of "detection limits" to flameless atomization devices has been questioned because of the "baseline upset" encountered whenever a blank is analyzed (2). This baseline upset has been attributed to deformation of the graphite furnace at high temperatures, residual analyte, and imperfect alignment of the background corrector. With the CEWM-AA system, detection limit measurements can be made without these problems. Since  $I_0$  is defined as the source intensity on both sides of the analyte line, the reference and the analyte wavelengths are both present in the single beam which passes through the furnace. Graphite deformation will affect  $I_0$  and  $I$  in an identical manner. Residual analyte, which may exist on the graphite tube or end cones, can no longer make a contribution when the monochromator is tuned off the analyte line. Finally, since a single source is used, there can be no such thing as an imperfectly aligned background corrector. As a result, using off-the-line background noise levels, a valid detection limit can be calculated for standards and samples, regardless of the matrix, as shown in Table I.

The background noise levels for Cd in aqueous and complex matrices constitutes a near "worst case" situation for CEWM-AA. This is mostly due to the comparatively low intensity of the Eimac source at this wavelength (228.8 nm). The Eimac source gives a photocathode current 100 times larger at its most intense wavelength ( $\sim$ 480.0 nm) (23). As

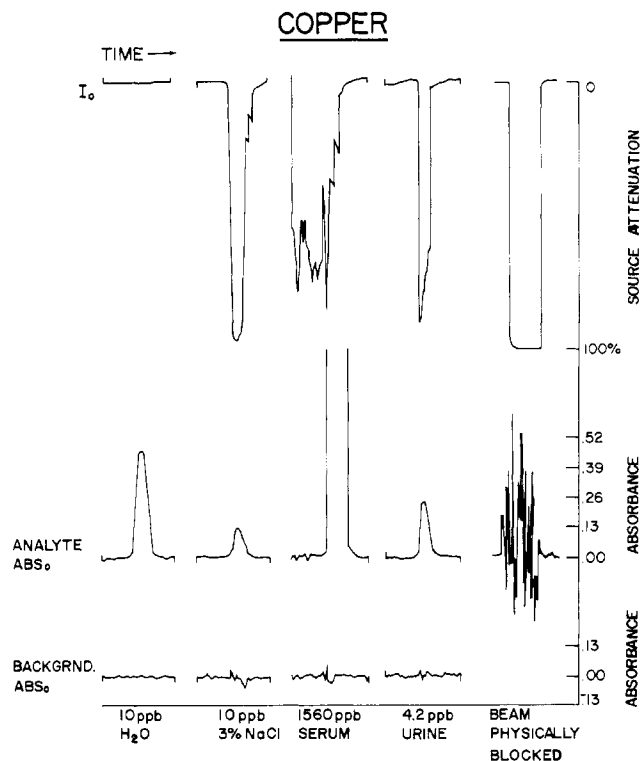


**Figure 7.** Traces of  $I_0$ , analyte absorbance, and background absorbance noise (off the line) for the analysis of Cu in  $H_2O$ , 3% NaCl, serum, and urine (100- $\mu$ L sample size)

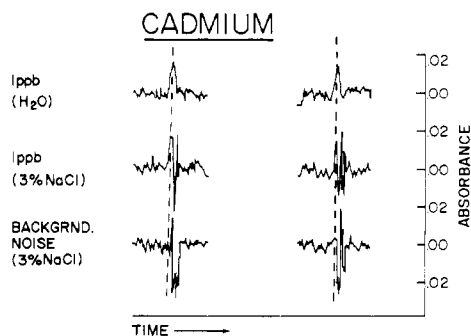


**Figure 8.** Traces of analyte absorbance and background absorbance noise (off the line) for duplicate analyses of Cd in  $H_2O$  and 3% NaCl

a result, elements at higher wavelengths show lower background noise levels. This can be seen readily upon comparing Cd to Cu (324.7 nm, Figure 7 and Table II) or Pb (283.3 nm, Table III).

Particular care must be taken in the measurement of the background noise levels. First, the accuracy of the determination of the peak-to-peak noise levels is very poor when based on a single analysis. The values listed in this paper represent an average of five determinations. In addition, as was pointed out earlier for Cd, the analyte absorbance peak may precede or trail the major noise component. Consequently detection limits, as reported in this paper, are conservative because they are based on the maximum background noise levels. This can be seen for 1 ppb Cd in 3% NaCl in Figure 8. Based on the maximum background noise levels, the detection limit is 2 ppb. However, 1 ppb is readily distinguished as the peak which precedes the noise component. With a little care, an effective detection limit below 1 ppb could be realized.

More accurate detection limits could be determined if the noise levels were known at the moment of peak analyte absorbance. Alternatively, if  $I_0$  were known at the peak

**Table IV.** Background Corrected Detection Limits (pg): Aqueous Matrices

	Conventional (6)	ZAA (20)	CEWM-AA <sup>a</sup>
Cd (2288)	0.1	0.3	4
Pb (2170)	5	...	...
(2833)	...	4	22
Cu (3247)	5	10	7
Atomizer	CRA-63	Zeeman Furnace	HGA-2000

<sup>a</sup> This work.

absorbance, the noise levels could be calculated with reasonable accuracy (Figure 5).

Tables I, II, and III show the results obtained for the analysis of Cd, Pb, and Cu in  $H_2O$ , 3% NaCl, serum, and urine. For Cu, a 100- $\mu$ L sample size was also used in addition to the 20- $\mu$ L samples in order to determine whether or not the improved background correction capability would allow larger samples to be used to reduce concentration detection limits. As expected, all elements show a degradation of the detection limits in the complex matrices, as a result of the increased background noise levels and matrix suppression interferences. The slope of the analytical curve was calculated for each solution in terms of milliabsorbance/pg and can be used as an indicator of the severity of the matrix suppression effect. The data for the 100- $\mu$ L Cu samples show that the atomization efficiency of the atomizer is reduced with such large samples, with the result that the expected improvement in the concentration detection limit with larger sample size is not observed.

**Comparison of Background Correction Systems.** It is difficult to compare the CEWM-AA system directly to commercially available background corrected AA instruments because of the dearth of published information. The data that are available must be considered carefully because of the different atomization sources and sample matrices used.

The parameter most frequently considered is the maximum source attenuation by the matrix that an instrument can tolerate. Pye Unicam (10) and Hitachi (17) both quote a limit of 1.7 absorbance units for their instruments. CEWM-AA, as discussed earlier can tolerate 3.0 absorbance units of attenuation. Attenuation limits for other commercial instruments are not available. It would be informative to compare detection limits for aqueous solutions analyzed in the background corrected mode. However, with the exception of the Hitachi ZAA instrument, for which background correction is an inherent feature, no detection limits of this nature have been published by any manufacturers of AA instruments. For conventional background corrected line source instruments (AAL-BC), the data reported by Donnelly et al. (6) represents the only information that could be found. The comparative data are shown in Table IV. CEWM-AA is approximately an order of magnitude worse for Cd and a factor of 3 to 4 worse for Pb when detection limits are compared to those for ZAA and AAL-BC. This comparison reflects the relatively low intensity of the Eimac VIX-UV lamp in the UV region. For Cu, CEWM-AA has detection limits only a factor of 2 worse than those for AAL-BC and fractionally better than ZAA detection limits. It must be remembered, however, that a different atomization source was used with each of the three systems.

Detection limits in a high salt matrix provide a more realistic comparison of the background correction capabilities of the instruments. Unfortunately, no data of this nature are available from any of the manufacturers of AA instruments. Detection limits for a Perkin-Elmer 303 equipped with a  $D_2$  lamp and an HGA 2000 graphite furnace have been reported by Cruz and Van Loon (34). Detection limits for a ZAA system

Table V. Background Corrected Detection Limits (pg): High Salt Matrices

Matrix	Conventional (34) Varied	ZAA (40) 3% NaCl	CEWM-AA <sup>a</sup> 3% NaCl
Cd (2288)	40	...	40
Pb (2170)	200	...	...
(2833)	...	350	100
Cu (3247)	240	50	50
Atomizer	HGA-2000	... <sup>b</sup>	HGA-2000

<sup>a</sup> This work. <sup>b</sup> Self-built furnace.

employing the magnetic field around the light source were calculated from analytical traces published by Hadeishi and McLaughlin (40). These detection limits are compared to the detection limits for CEWM-AA in Table V. CEWM-AA is comparable to or better than ZAA and AAL-BC for every element. Unfortunately, Gruz and Van Loon (34) employed different salt matrices. Close examination of their data shows that they encountered less source attenuation but a slightly greater matrix suppression effect. Consequently, a rough comparison of the data for all three systems appears justifiable.

### LITERATURE CITED

- (1) S. R. Koertyohann and E. E. Pickett, *Anal. Chem.*, **28**, 585 (1966).
- (2) H. L. Kahn, M. Bancroft, and R. H. Emmel, *Res/Dev.*, **27**, 30 (1976).
- (3) D. C. Manning, *At. Absorp., Newsl.*, **11**, 112 (1972).
- (4) C. Hendrikx-Jongerius and L. De Galan, *Anal. Chim. Acta*, **87**, 259 (1976).
- (5) A. T. Zander, *Am. Lab.*, **8**, 11 (1976).
- (6) T. H. Donnelly, J. Ferguson, and A. J. Eccleston, *Appl. Spectrosc.*, **29**, 158 (1975).
- (7) L. Morgenthaler, *Am. Lab.*, **4**, 41 (1975).
- (8) "Atomic Absorption Methods Manual, Volume II, Flameless Operations", Instrumentation Laboratory (1976).
- (9) "Instructions, Model 603, Atomic Absorption Spectrophotometer" (993-9208) March 1976.
- (10) L. R. Morris and R. A. Newstead, "Improved Background Correction for AAS", Paper No. 97, Pittsburgh Conference on Analytical Chemistry and Applied Spectroscopy, Cleveland, Ohio, 1977.
- (11) L. R. Morris and R. A. Newstead, "A Compact Double Beam AAS", Paper No. 102, Pittsburgh Conference on Analytical Chemistry and Applied Spectroscopy, Cleveland, Ohio, 1977.
- (12) K. C. Thompson and R. G. Godden, *Analyst (London)*, **101**, 96 (1976).
- (13) J. Y. Marks, R. J. Spellman, and G. Wysocki, *Anal. Chem.*, **48**, 1474 (1976).

- (14) J. Y. Marks and G. G. Welcher, Paper No. 176, 3rd Annual Meeting of FACSS, Philadelphia, Pa., 1976.
- (15) A. T. Zander, T. C. O'Haver, and P. N. Keliher, *Anal. Chem.*, **49**, 838 (1977).
- (16) H. Koizumi and K. Yasuda, *Anal. Chem.*, **47**, 1679 (1975).
- (17) H. Koizumi and K. Yasuda, *Anal. Chem.*, **48**, 1178 (1976).
- (18) H. Koizumi and K. Yasuda, *Spectrochim. Acta, Part B*, **31**, 237 (1976).
- (19) H. Koizumi and K. Yasuda, *Spectrochim. Acta, Part B*, **31**, 523 (1976).
- (20) H. Koizumi, K. Yasuda, and M. Katayama, *Anal. Chem.*, **49**, 1106 (1977).
- (21) W. Snelleman, *Spectrochim. Acta, Part B*, 403 (1968).
- (22) R. N. Hager, Jr., *Anal. Chem.*, **45**, 1131A (1973).
- (23) A. T. Zander, T. C. O'Haver, and P. N. Keliher, *Anal. Chem.*, **48**, 1166 (1976).
- (24) P. N. Keliher and C. C. Wohlers, *Anal. Chem.*, **48**, 140 (1976).
- (25) S. R. Koertyohann, E. D. Glass, D. A. Yates, E. J. Hinderberger, and F. E. Lichte, *Anal. Chem.*, **49**, 1121 (1977).
- (26) M. S. Epstein and T. C. O'Haver, *Spectrochim. Acta, Part B*, **30**, 135 (1975).
- (27) R. Sydor and G. M. Hieftje, *Anal. Chem.*, **48**, 2030 (1976).
- (28) R. C. Elser and J. D. Winefordner, *Spectrochim. Acta, Part B*, **23**, 403 (1968).
- (29) G. J. Nitis, V. Svoboda, and J. D. Winefordner, *Spectrochim. Acta, Part B*, **27**, 345 (1972).
- (30) C. Veillon and P. Merchant, Jr., *Appl. Spectrosc.*, **27**, 361 (1973).
- (31) M. D. Amos, P. A. Bennet, K. G. Brodie, P. W. Y. Lung, and J. P. Matoušek, *Anal. Chem.*, **43**, 211 (1971).
- (32) J. Y. Hwang, P. A. Ullucci, S. B. Smith, Jr., and A. L. Malenfant, *Anal. Chem.*, **43**, 1319 (1971).
- (33) D. A. Segar and J. G. Gonzalez, *Anal. Chim. Acta*, **58**, 7 (1972).
- (34) R. B. Cruz and J. C. Van Loon, *Anal. Chim. Acta*, **72**, 231 (1974).
- (35) R. D. Ediger and J. D. Keiber, *At. Absorp. Newsl.*, **13**, 61 (1974).
- (36) F. Perry, S. R. Koertyohann, and M. Perry, Jr., *Clin. Chem. (Winston-Salem, N.C.)*, **21**, 626 (1975).
- (37) F. J. Ferrandez, *Clin. Chem. (Winston-Salem, N.C.)*, **21**, 558 (1975).
- (38) T. C. O'Haver, M. S. Epstein, and A. T. Zander, *Anal. Chem.*, **49**, 458 (1977).
- (39) "Analytical Methods for AAS Using the HGA Graphite Furnace", Perkin-Elmer (990-9972), March 1973.
- (40) T. Hadeishi and R. D. McLaughlin, *Science*, **187**, 348 (1975).

RECEIVED for review July 27, 1977. Accepted August 29, 1977. Presented in part at the 28th Pittsburgh Conference, Cleveland, Ohio, 1977. From a Dissertation to be submitted to the Graduate School, University of Maryland, by J. M. Harnly, in partial fulfillment of the requirements for the Ph.D. Degree in Chemistry. Financial support provided by USDA, Agricultural Research Service, Nutrient Composition Laboratory.

## Cumulative Sum Charts for Monitoring of Radioactivity Background Count Rates

Roger A. G. Marshall

School of Chemistry, Thames Polytechnic, Woolwich, London SE18 6PF, United Kingdom

Cumulative summation is a simple statistical technique which could be applied more widely in analytical chemistry. The background count rate of a radiochemical counter has been examined as an illustration of its use. The variation in the level of the background can contribute significantly to the error of radioactive measurements. However, when a number of samples of low activity have to be counted, the error may be minimized by initially estimating the background very accurately and thereafter assuming it to be constant. It is recommended that the constancy of the background count rate be then monitored using a cumulative sum chart. This will indicate comparatively rapidly when abrupt changes in the count rate of the order of one standard deviation of the measurement have occurred. The precise point at which the change occurred can also often be deduced and, if necessary, the results can be corrected retrospectively.

It is impossible to measure the activity of a radioactive source without simultaneously recording the background radiation and counter noise. An estimate of the background count rate ( $R_b$ ) is made in the absence of the source and subtracted from the total source plus background count rate ( $R_t$ ) to obtain that for the source alone ( $R_s$ ), i.e.,

$$R_s = R_t - R_b \quad (1)$$

Thus the error in the estimate of the background ( $\sigma_b$ ) must be added to that of the total source plus background ( $\sigma_t$ ) to obtain the sample error ( $\sigma_s$ ) according to the standard equation for the propagation of independent error (1):

$$\sigma_s = \sqrt{(\sigma_t^2 + \sigma_b^2)} \quad (2)$$

There are many sources of error in counting such as self-absorption, backscatter, and geometric effects, which are